Supporting information for:

Prediction of the ground state for indenofluorene-type systems with Clar's π-sextet model

Gibu George,[a] Anton J. Stasyuk,*[a,b,c] and Miquel Solà*[a]

[a] Institut de Química Computacional i Catàlisi and Departament de Química, Universitat de Girona, C/ Maria Aurèlia Capmany 69, 17003 Girona, Catalonia, Spain

[b] Faculty of Chemistry, University of Warsaw, Pasteura 1, 02-093 Warsaw, Poland

[c] Departament de Farmàcia i Tecnologia Farmacèutica, i Fisicoquímica, Facultat de Farmàcia i Ciències de l'Alimentació & Institut de Química Teòrica i Computacional (IQTCUB), Av. Joan XXIII 27-31, Universitat de Barcelona (UB), Barcelona, Spain

Abstract

This study introduces the Ground State Stability (GSS) rule that allows predicting the nature of the ground state of indenofluorene (**IF**)-type systems from the simple counting of the Clar π-sextets in the closed- and open-shell configurations. The **IF**-type system exhibits a triplet ground state when acquiring double or more the number of Clar π-sextet in the open-shell form relative to the closed-shell form; otherwise, it assumes an open-shell singlet ground state. Performed state-of-the-art DFT calculations and analysis of aromaticity for the systems of interest validate the effectiveness of the proposed rule. We demonstrate that aromaticity plays the most crucial role in determining the ground electronic state for such polycyclic hydrocarbons. The simplicity of the GSS rule makes it a robust strategy for identifying promising systems in the development of indenofluorene-type materials.

Table of Contents

Computational details

The biradical character index (y_0) was calculated following the Yamaguchi's scheme:[1]

$$y_0 = 1 - \left(\frac{2T}{1 + T^2}\right)$$

where,

$$T = \frac{n_{HOMO} - n_{LUMO}}{2}$$

n_{HOMO} and n_{LUMO} are the occupation numbers of the HOMO and LUMO levels respectively.[2] The range of biradical index goes from y_0 = 0 for pure closed-shell (CS) structure to y_0 = 1 for pure diradical. Additionally, we employed the fractional occupation number weighted density (FOD) method[3] to quantitatively evaluate the open-shell (OS) singlet biradical character which measures the appearance of “hot” electrons or strongly correlated electrons in a molecule. It is a measure of static electron correlation that uses finite temperature (FT)-DFT with pre-defined electronic temperature (T_{el}) for smearing the electrons of the molecule over the molecular orbitals.[4] N^{FOD} value from the FOD analysis is used as a descriptor of OS character and it quantifies the number of unpaired electrons to be correlated, indicative of a polyradical character. The ρ^{FOD} plots were visualized using the isocontour value of 0.02 e Bohr^{-3}.

Aromaticity analyses were carried out using the same level of theory for geometry optimizations. The delocalization of electrons was evaluated using the electron density of the delocalized bonds (EDDB)[5] method. EDDB analysis represents different levels of electron delocalization, such as the electron density localized on the atoms (EDLA), the electron density localized on the bonds (EDLB), and the EDDB which characterizes the electron density that cannot be assigned to either atoms or bonds due to its multicenter delocalized nature. We used the population of electrons from EDDB through all the conjugated bonds in the ring as a descriptor for aromaticity. EDDB analyses were performed using RunEDDB code involving the Hilbert-space partitioning within the representation of natural atomic orbitals using the NBO 7.0 software.[6] The π-EDDB values studied in this work were normalized by the total number of π-electrons involved in the delocalization. The calculation of multicenter delocalization index (MCI)[7] employs the Quantum Theory of Atoms in Molecules[8] for atomic partitioning, performed using the AIMAll software[9]. The resulting atomic overlap matrices from this partition, along with the wavefunction files serve as inputs for the ESI-3D code[10], which provides the MCI values.

For the magnetic criteria, we performed the out-of-plane two-dimensional nucleus independent chemical shift (2D-NICS) scan along the XY plane of the molecule using a two-dimensional grid of dummy atoms placed 1Å above the plane.[11] 3D-NICS was calculated by generating 3D grids of different sizes depending on the studied molecules. Each point in this grid was placed by dummy atoms located 0.25 Å one from another in three spatial directions. NICS was calculated using the GIAO (Gauge Including Atomic Orbitals)[12] method and the $NICS(1)_{zz}$ values are defined as the negative zz-component of the shielding tensor at 1Å above the molecular plane. $NICS(0)_{iso}$ values were computed by analyzing the isotropic magnetic shielding calculated at the center of the ring plane. NICS-XY scan were analyzed by placing the NICS probes at a height of 1.7 Å above the system with an interval of 0.2 Å.[13] Negative NICS value represents a diatropic ring current and a positive value represents a paratropic ring current indicative of aromatic and antiaromatic character, respectively. The magnetically induced current densities was carried out by means of GIMIC program[14] and the calculations were performed using GIAO method.[15] In the current density plots, the intensity of current decreases going from light yellow (0.4 $nA \cdot T^{-1} \cdot Å^{-2}$) to red and black ($4 \cdot 10^{-5}$ $nA \cdot T^{-1} \cdot Å^{-2}$), and the black arrows indicate the direction of the current flow), and the black arrows indicate the direction of the current flow. According to the normal convention, the diatropic current is represented by the current flowing in clockwise direction, while a paratropic current is represented by the current flowing in counterclockwise direction.

Table S1. T_1 diagnostic for **IF** systems computed at the DLPNO-CCSD(T)/cc-pVTZ level of theory.

	T_1 diagnostic	
Systems	**Singlet**	**Triplet**

IF-1a	0.0113	0.0186
IF-1b	0.0108	0.0177
IF-2a	0.0112	0.0186
IF-2b	0.0107	0.0182
IF-2c	0.0108	0.0186

Table S2. The calculated relative energies (kcal/mol) of isomers of **FF** in different electronic states and their singlet-triplet energy gap ($\Delta E_{S\text{-}T}$), the diradical character (y_0) and the N^{FOD} values computed at the (U)LC-ωPBE/def2-TZVPP level of theory.

Systems	*E* (CS)	*E* (T)	*E* (OSS)	$\Delta E_{S\text{-}T}$ [a]	y_0	N^{FOD}	Ratio [b]
FF-1a	0.00	-23.00	-20.96	2.04	0.69	1.55	1:3 (3)
FF-1b	0.00	0.30	-6.92	-7.23	0.31	1.10	2:3 (1)
FF-2a	0.00	0.14	-6.50	-6.64	0.31	1.22	2:3 (1)
FF-2b	0.00	-25.52	-21.63	3.89	0.92	1.96	1:3 (3)
FF-2c	0.00	-25.29	-21.48	3.81	0.95	2.01	1:3 (3)
FF-2d	0.00	-3.85	-9.17	-5.32	0.43	1.42	2:3 (1)
FF-3a	0.00	-7.10	-12.02	-4.91	0.55	1.66	2:3 (1)
FF-3b	0.00	-24.95	-20.62	4.33	0.84	1.94	1:3 (3)
FF-3c	0.00	1.84	-6.19	-8.04	0.28	1.19	2:3 (1)
FF-4a	0.00	-28.57	-23.98	4.59	0.99	2.19	1:3 (3)
FF-4b	0.00	-1.33	-7.58	-6.25	0.38	1.42	2:3 (1)
FF-4c	0.00	-22.01	-18.56	3.45	0.71	1.77	1:3 (3)

[a] $\Delta E_{S\text{-}T}$ = *E*(OSS) - *E*(T). [b] the ratio of number of Clar π-sextets between the ground state OS and CS resonance structures. The number in parentheses represents the spin multiplicity of this ground OS electronic state.

Table S3. The calculated relative energies (kcal/mol) of isomers of **DIAn** in different electronic states and their singlet-triplet energy gap ($\Delta E_{S\text{-}T}$), the diradical character (y_0) and the N^{FOD} values computed at the (U)LC-ωPBE/def2-TZVPP level of theory.

Systems	*E* (CS)	*E* (T)	*E* (OSS)	$\Delta E_{S\text{-}T}$ [a]	y_0	N^{FOD}	Ratio [b]
DIAn-1a	0.00	-30.74	-27.70	3.05	0.81	1.74	1:3 (3)
DIAn-1b	0.00	-8.13	-13.62	-5.49	0.51	1.40	2:3 (1)
DIAn-2a	0.00	-33.25	-28.93	4.32	0.92	1.98	1:3 (3)
DIAn-2b	0.00	-11.64	-16.33	-4.69	0.61	1.65	2:3 (1)
DIAn-2c	0.00	-34.48	-30.61	3.87	0.91	1.97	1:3 (3)
DIAn-2d	0.00	-7.23	-12.98	-5.75	0.49	1.49	2:3 (1)
DIAn-3a	0.00	-14.47	-19.10	-4.62	0.69	1.86	2:3 (1)
DIAn-3b	0.00	-36.53	-31.66	4.87	0.95	2.22	1:3 (3)
DIAn-3c	0.00	-5.58	-12.49	-6.91	0.47	1.55	2:3 (1)
DIAn-4a	0.00	-35.18	-30.92	4.26	0.99	2.26	1:3 (3)
DIAn-4b	0.00	-10.17	-15.63	-5.46	0.59	1.74	2:3 (1)
DIAn-4c	0.00	-33.07	-27.88	5.19	0.89	2.13	1:3 (3)

[a] $\Delta E_{S\text{-}T} = E(\text{OSS}) - E(\text{T})$. [b] the ratio of number of Clar π-sextets between the ground state OS and CS resonance structures. The number in parentheses represents the spin multiplicity of this ground OS electronic state.

Table S4. Normalized π-EDDB values of all the systems studied in CS and OS (triplet or singlet based on the stability).

Systems	normalized π-EDDB values (*e*)	
	CS	**OS** [a]
IF-1a	0.52	0.80 (3)
IF-1b	0.65	0.67 (1)
IF-2a	0.48	0.79 (3)
IF-2b	0.65	0.69 (1)
IF-2c	0.64	0.65 (1)
FF-1a	0.54	0.76 (3)
FF-1b	0.60	0.74 (1)
FF-2a	0.60	0.72 (1)
FF-2b	0.49	0.78 (3)
FF-2c	0.49	0.76 (3)
FF-2d	0.61	0.77 (1)
FF-3a	0.62	0.79 (1)
FF-3b	0.49	0.77 (3)
FF-3c	0.60	0.71 (1)
FF-4a	0.50	0.79 (3)
FF-4b	0.60	0.76 (1)
FF-4c	0.51	0.75 (3)
DIAn-1a	0.53	0.76 (3)
DIAn-1b	0.57	0.75 (1)
DIAn-2a	0.53	0.75 (3)
DIAn-2b	0.58	0.76 (1)
DIAn-2c	0.54	0.76 (3)
DIAn-2d	0.57	0.73 (1)
DIAn-3a	0.59	0.78 (1)
DIAn-3b	0.53	0.76 (3)
DIAn-3c	0.57	0.72 (1)
DIAn-4a	0.50	0.78 (3)
DIAn-4b	0.58	0.75 (1)
DIAn-4c	0.51	0.74 (3)
IF-2b-ext-1	0.61	0.75 (1)
IF-2b-ext-2	0.68	0.73 (1)
IF-2b-ext-3	0.59	0.74 (1)
FF-1a-ext	0.67	0.80 (3)

FF-1b-ext	0.56	0.68 (1)
IF-1a-NT	0.51	0.68 (3)
IF-1b-NT	0.53	0.57 (1)
Coro-1a	0.67	0.76 (3)
Coro-1b	0.69	0.76 (1)
Cora-1a	0.69	0.71 (3)
Cora-1b	0.55	0.71 (3)
HPZ1	0.58	0.76 (1)
HPZ2	0.55	0.65 (1)
OCZ	0.58	0.78 (1)
BPaz	0.55	0.79 (3)
Az-NG	0.69	0.81 (1)

[a] The number in parentheses represents the spin multiplicity of ground OS electronic state.

Table S5. Comparison of difference in Clar π-sextet numbers and their ratio between the CS and OS systems.

Systems	**Ratio [a]**	**ΔClar [b]**
IF-1a	1:3 (3)	2
IF-1b	2:3 (1)	1
IF-2a	1:3 (3)	2
IF-2b	2:3 (1)	1
IF-2c	2:3 (1)	1
FF-1a	1:3 (3)	2
FF-1b	2:3 (1)	1
DIAn-1a	1:3 (3)	2
DIAn-1b	2:3 (1)	1
IF-2b-ext-1	2:3 (1)	1
IF-2b-ext-2	2:3 (1)	1
IF-2b-ext-3	2:3 (1)	1
FF-1a-ext	1:4 (3)	3
FF-1b-ext	2:3 (1)	1
IF-1a-NT	1:3 (3)	2
IF-1b-NT	2:3 (1)	1
Coro-1a	2:5 (3)	3
Coro-1b	3:5 (1)	2
Cora-1a	2:4 (3)	2
Cora-1b	2:4 (3)	2

HPZ1	2:3 (1)	1
HPZ2	2:3 (1)	1
OCZ	2:3 (1)	1
Az-NG	4:7 (1)	3
BPaz	1:3 (3)	2

[a] The ratio of number of Clar π-sextets between the ground state OS and CS resonance structures. The number in parentheses represents the spin multiplicity of this ground OS electronic state. [b] the difference in Clar's π-sextet numbers between the CS and the corresponding OS electronic state.

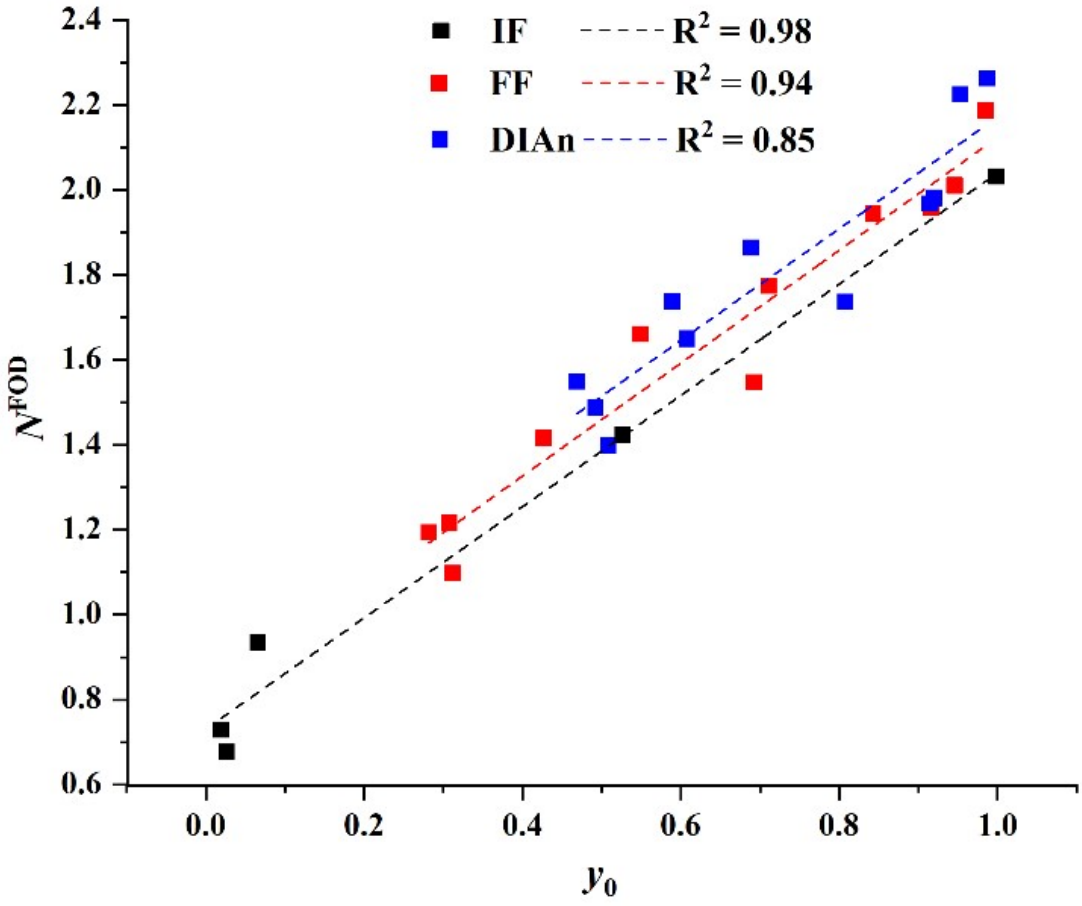

Figure S1. Relationship between calculated N^{FOD} and y_0 values for **IF**, **FF**, and **DIAn** structures, as well as corresponding correlation coefficients.

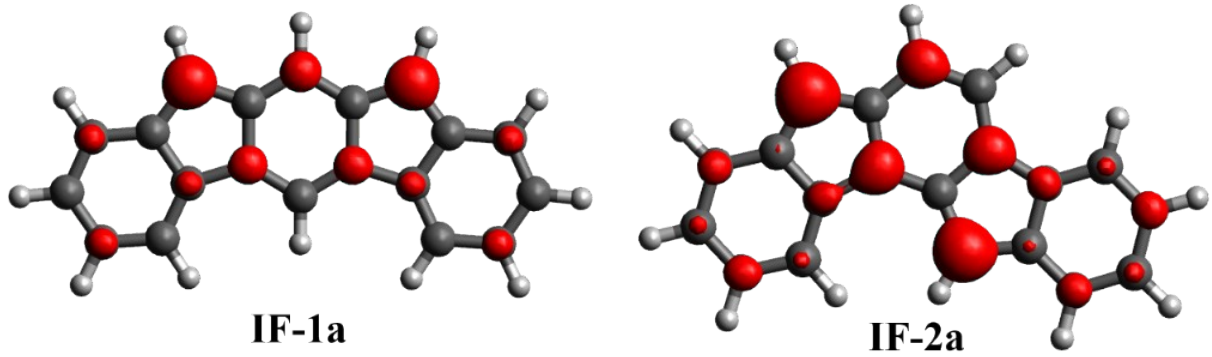

Figure S2. FOD plots for **IF-1a** and **IF-2a** at σ = 0.005 e Bohr^{-3} (TPSS/def2-TZVPP, T_{el} = 5000 K).

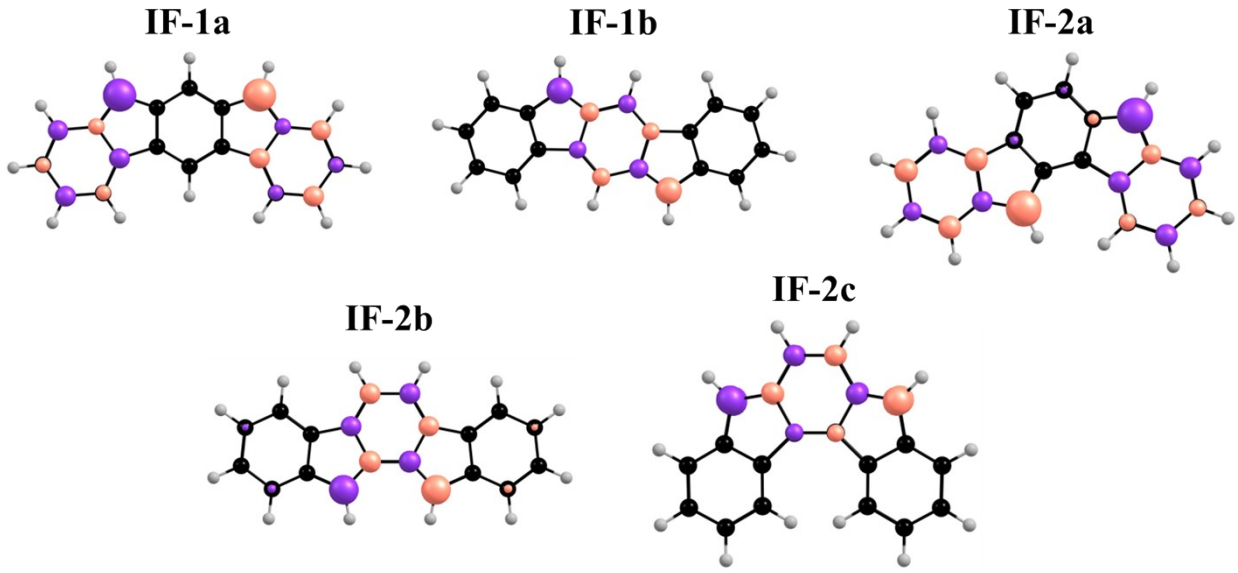

Figure S3. Spin density distribution (isovalue ρ = 0.015) of **IF** systems computed at (U)LC-ωPBE/def2-TZVPP level of theory.

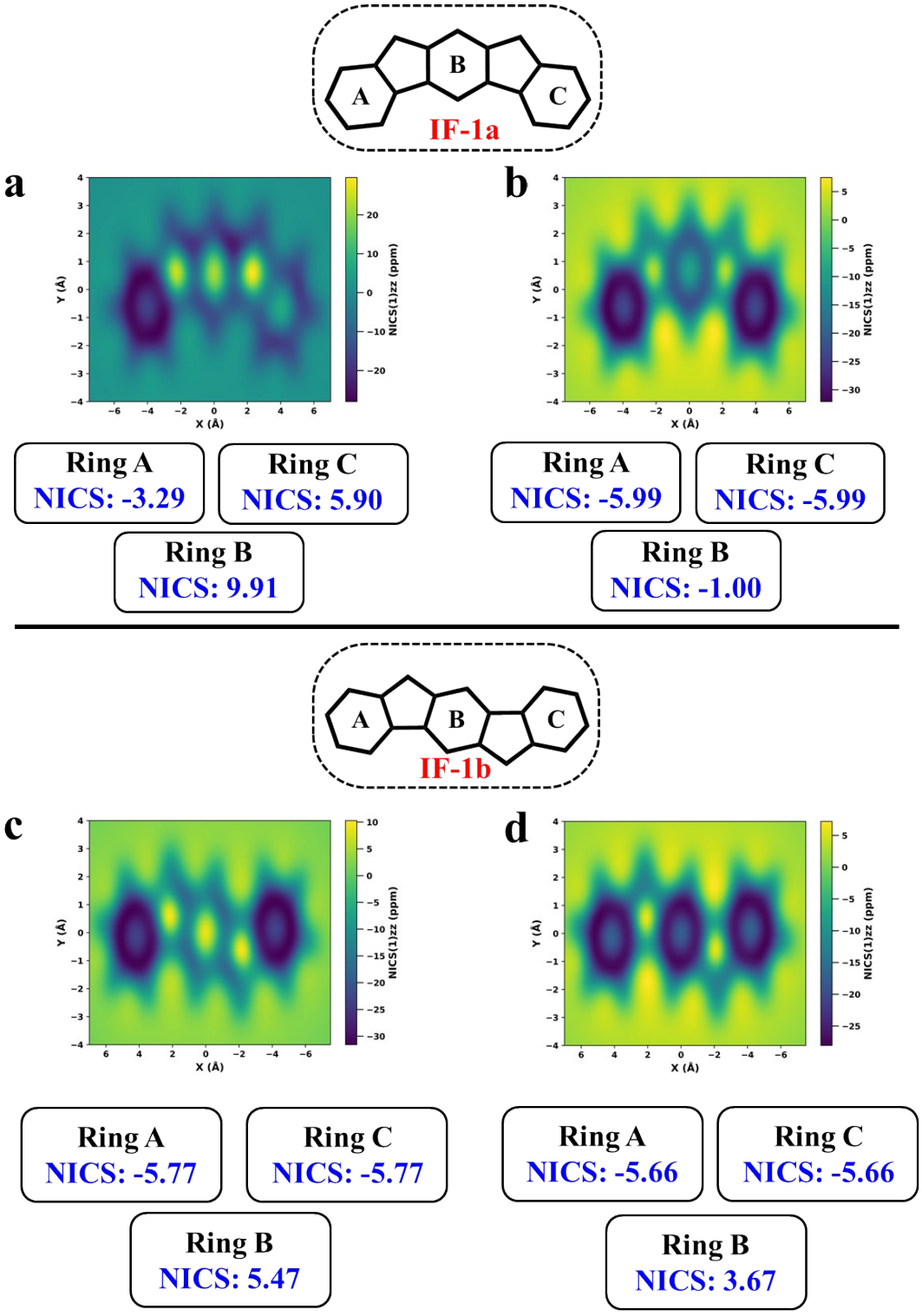

Figure S4. NICS(0)$_{iso}$ (in ppm) for CS (a)/(c), OS triplet (b) and singlet (d) states of **IF-1a** and **IF-1b**, as well as their corresponding 2D-NICS(1)$_{zz}$ scan.

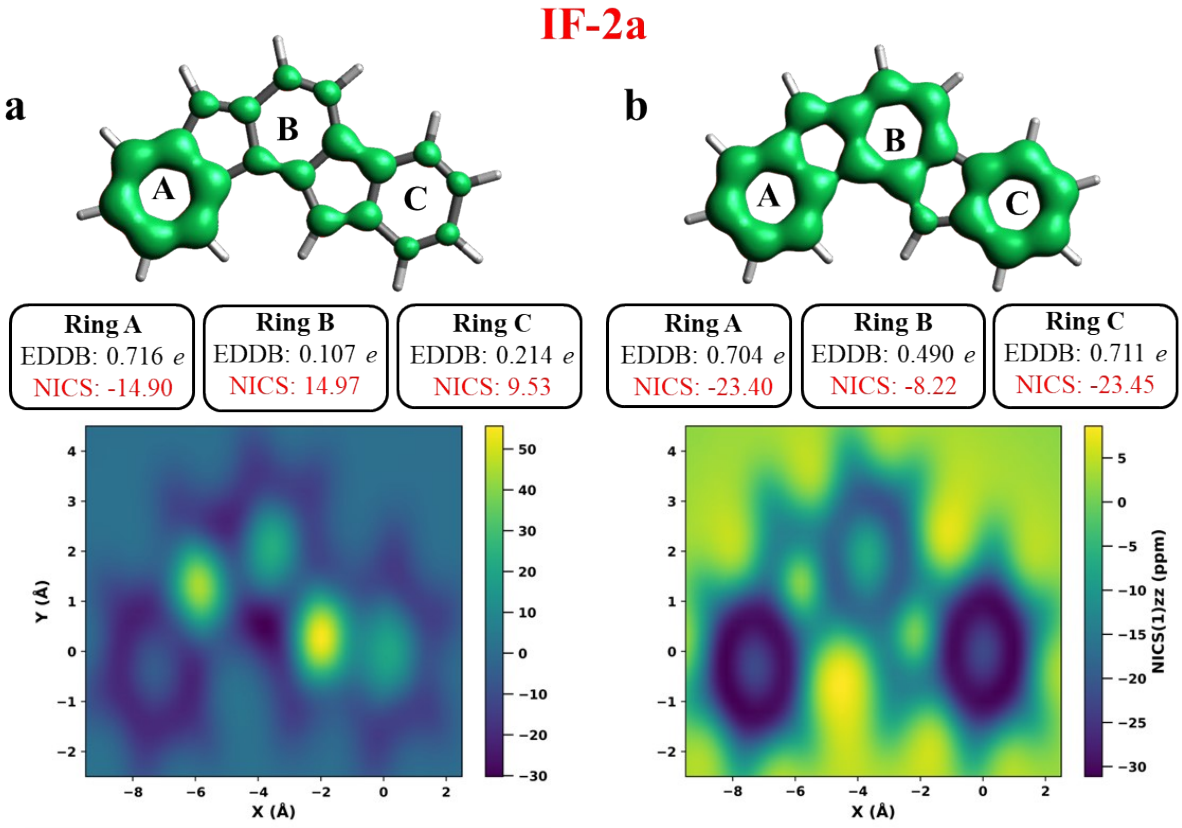

Figure S5. π-EDDB plots (isovalue: 0.015 e), normalized π-EDDB values and NICS(1)$_{zz}$ (in ppm) values for CS (a) and OS triplet state (b), as well as corresponding 2D-NICS(1)$_{zz}$ scan of **IF-2a**.

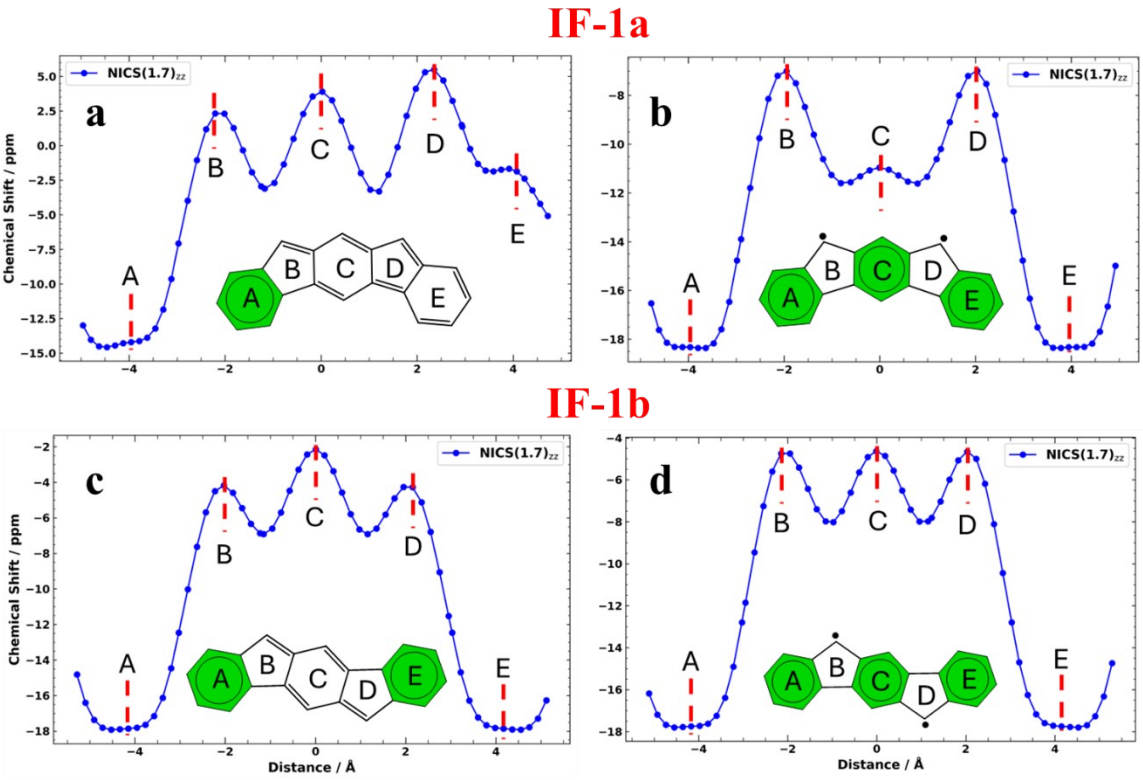

Figure S6. NICS-XY scan for CS (a)/(c), OS triplet (b) and singlet (d) states of **IF-1a** and **IF-1b** at a distance of 1.7 Å above the molecular plane.

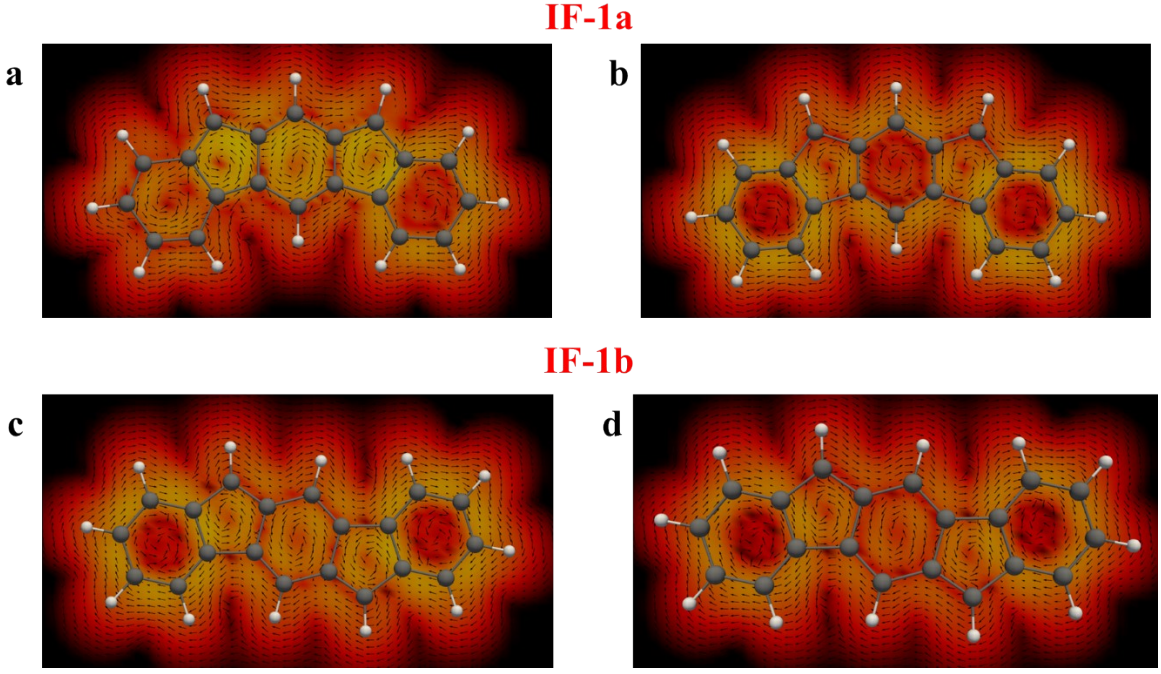

Figure S7. GIMIC plots (currents located 2 bohr above the molecular plane) for CS (a)/(c), OS triplet (b) and singlet (d) states of **IF-1a** and **IF-1b.** Currents in the perpendicular plane

with respect to the magnetic field located 2 bohr above the molecular plane. The intensity of current decreases going from light yellow (0.4 nA·T^{-1}·Å^{-2}) to red and black (4·10^{-5} nA·T^{-1}·Å^{-2}), and the black arrows indicate the direction of the current flow for the same states.

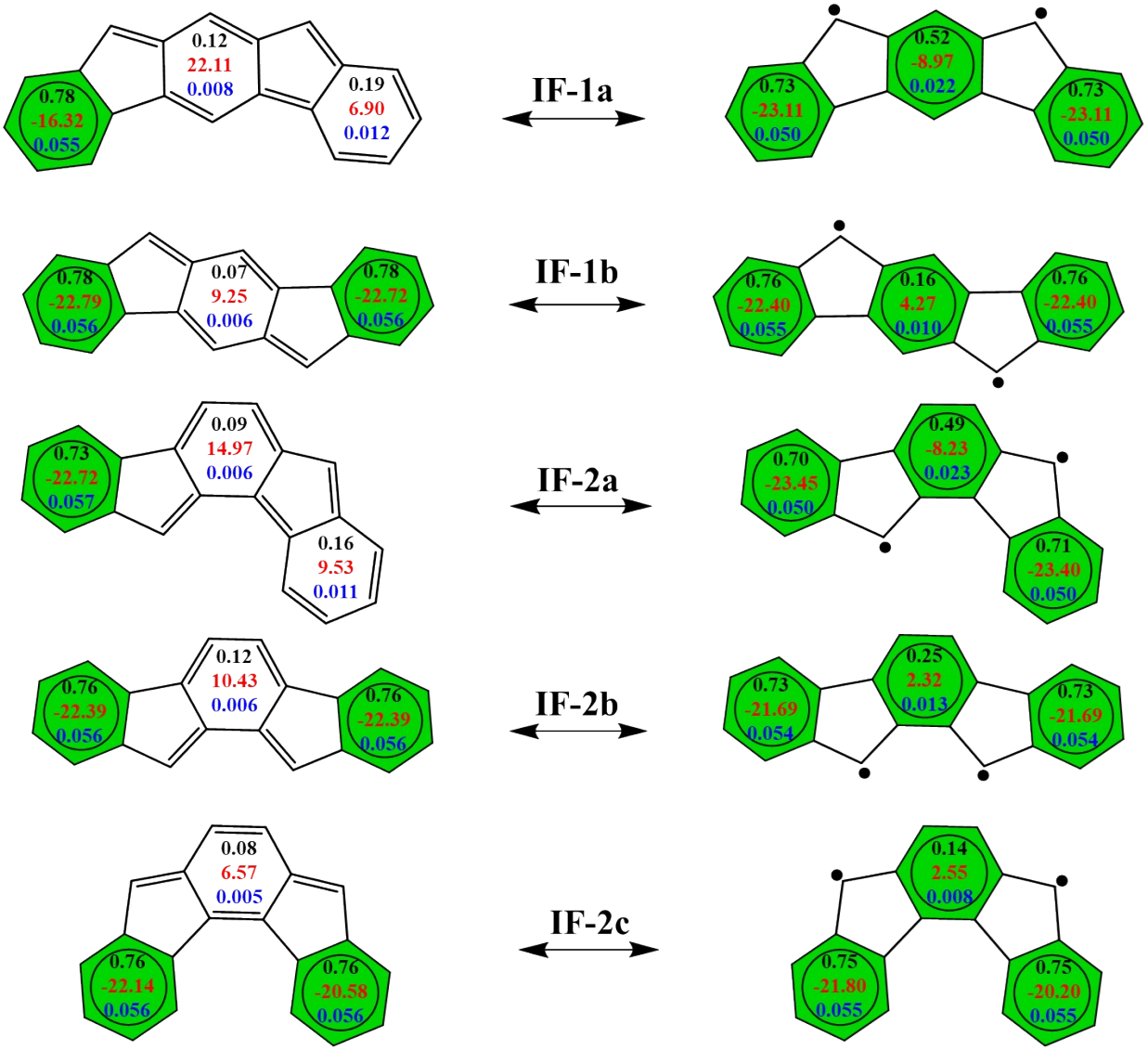

Figure S8. Normalized π-EDDB (numbers in black, electrons), NICS(1)$_{zz}$ (numbers in red, ppm) and MCI (numbers in blue, electrons) values for CS and OS forms of **IF** isomers. Ring with a green color indicative of the Clar's aromatic π-sextets.

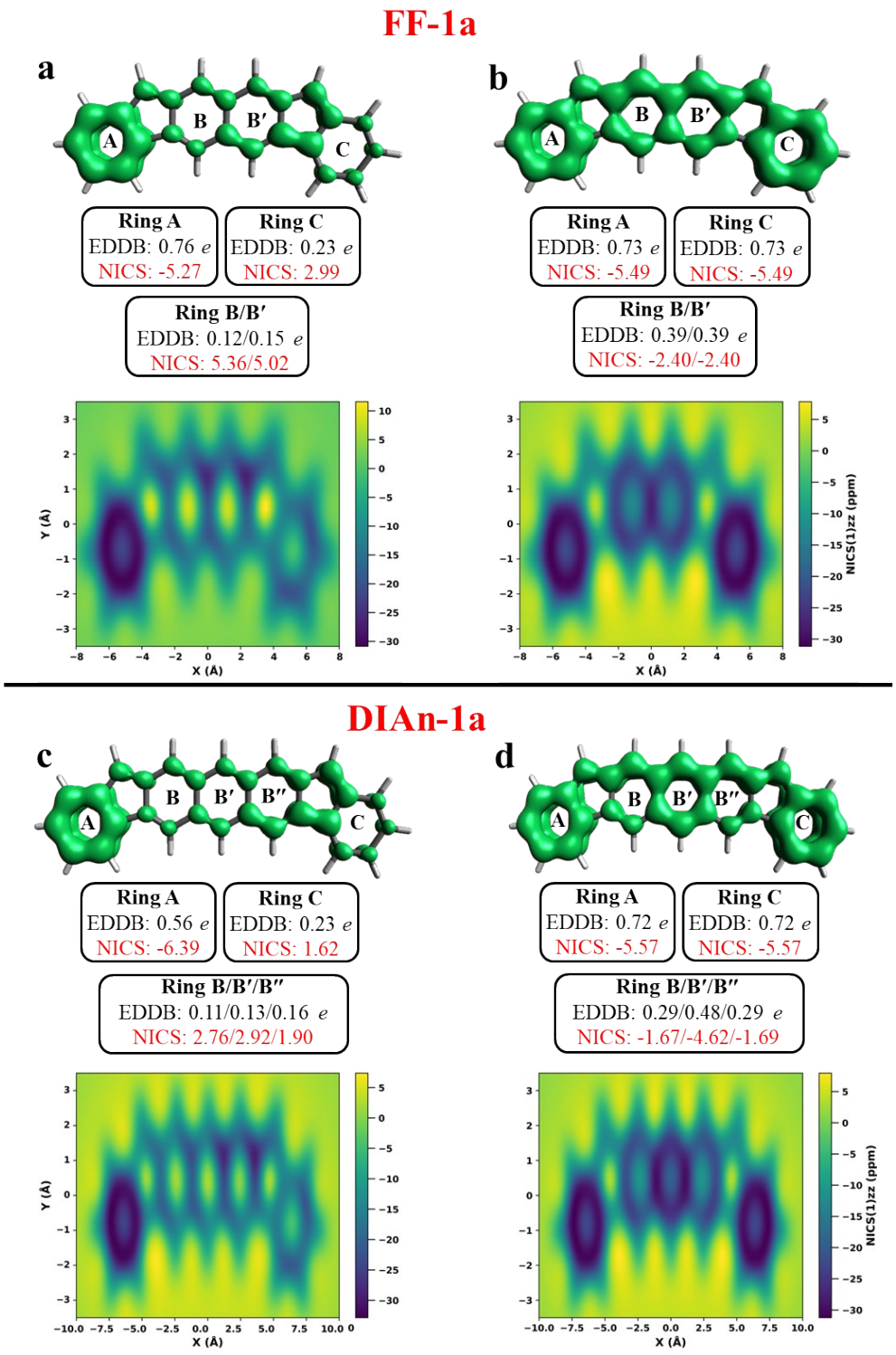

Figure S9. π-EDDB plots (isovalue: 0.015 e), normalized π-EDDB values, and NICS(0)$_{iso}$ (in ppm) values for CS (a)/(c) and OS triplet (b)/(d) states, as well as corresponding 2D-NICS(1)$_{zz}$ scan of **FF-1a** and **DIAn-1a**.

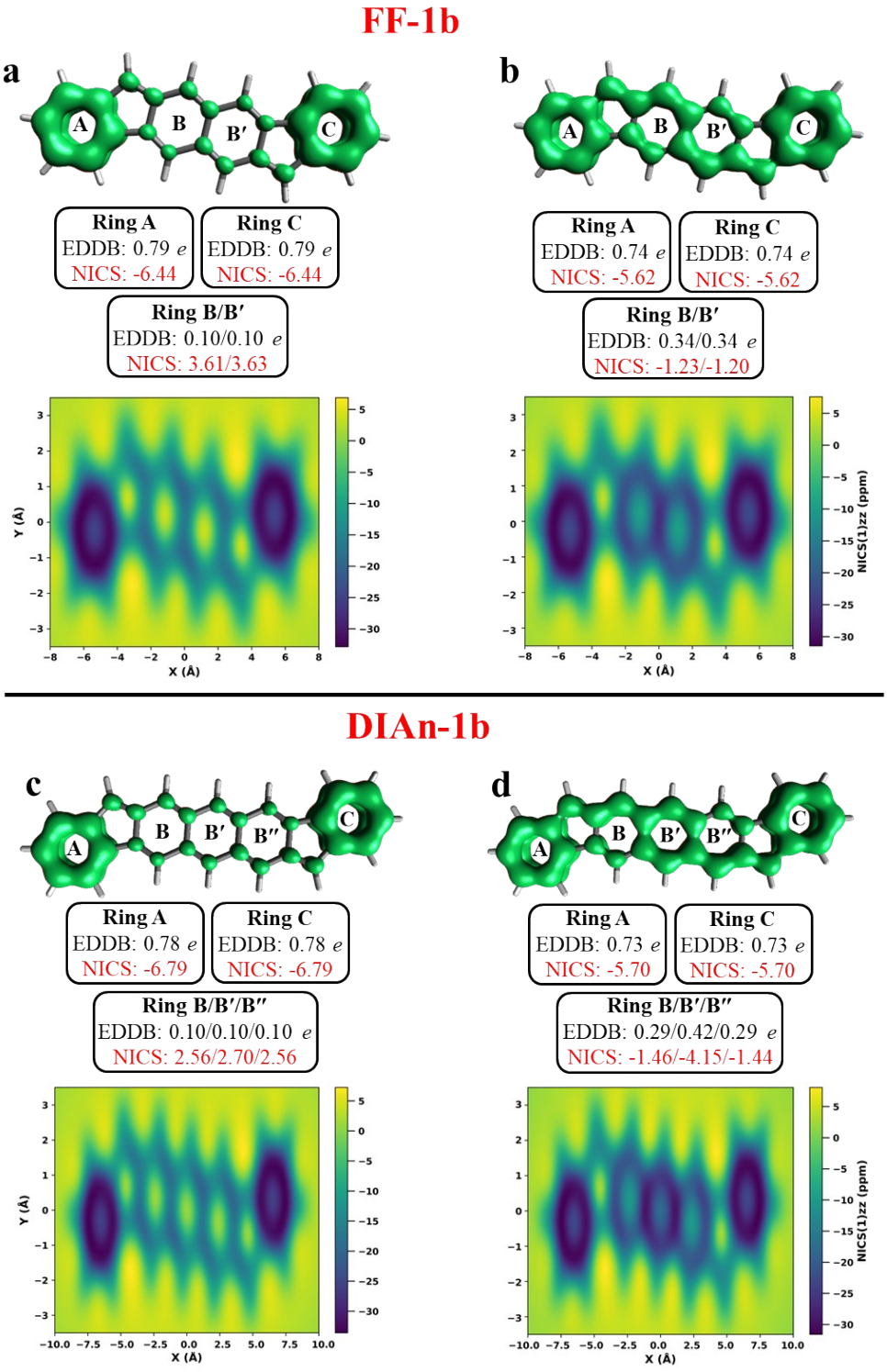

Figure S10. π-EDDB plots (isovalue: 0.015 e), normalized π-EDDB values, and NICS(0)$_{iso}$ (in ppm) values for CS (a)/(c) and OS singlet (b)/(d) states, as well as coresponding 2D-NICS(1)$_{zz}$ scan of **FF-1b** and **DIAn-1b**.

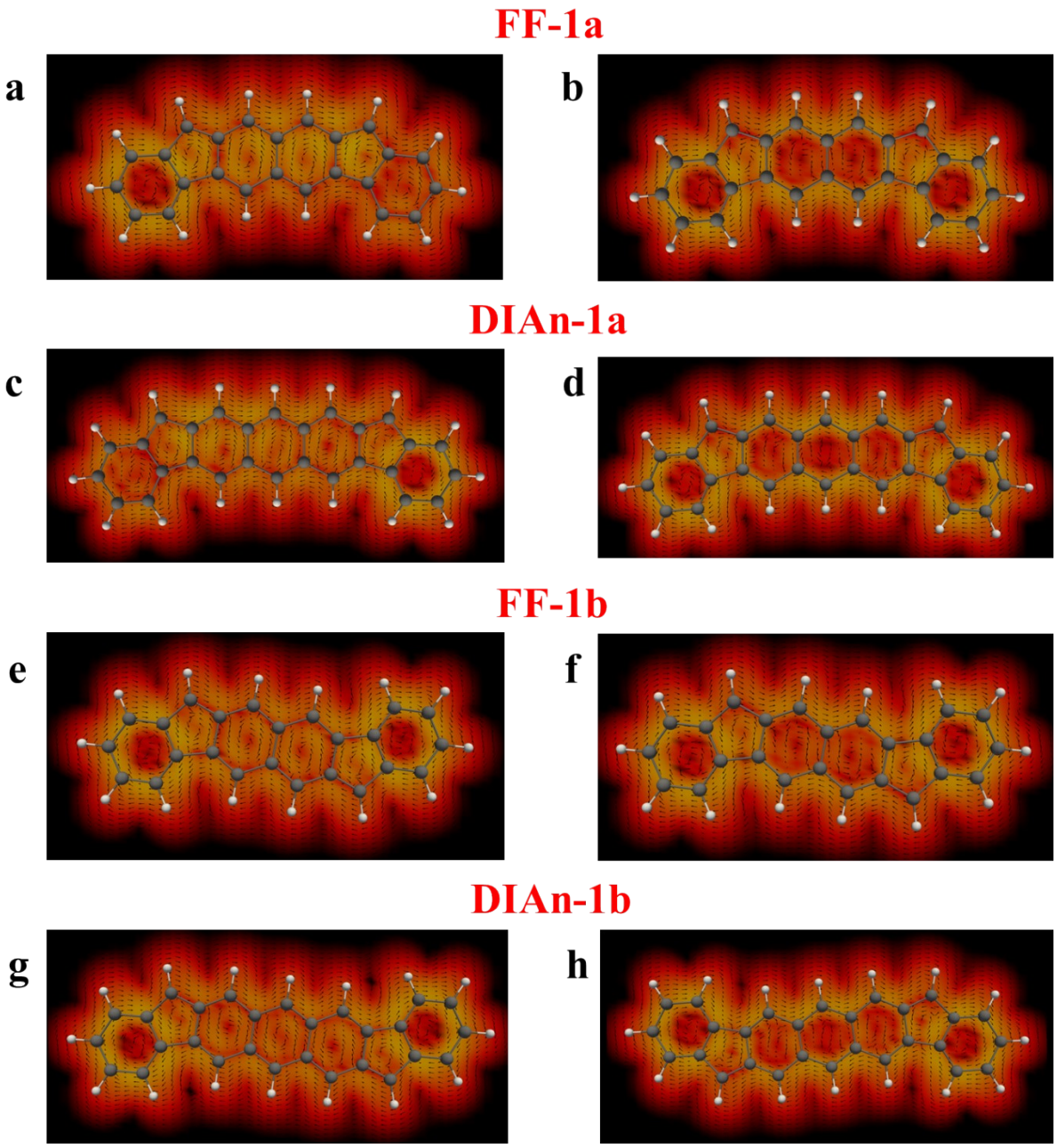

Figure S11. GIMIC plots for CS (a)/(c)/(e)/(g), OS triplet (b)/(d) and singlet (f)/(h) states of **FF-1a/1b** and **DIAn-1a/1b.** Currents in the perpendicular plane with respect to the magnetic field located 2 bohr above the molecular plane. The intensity of current decreases going from light yellow (0.4 $nA \cdot T^{-1} \cdot Å^{-2}$) to red and black ($4 \cdot 10^{-5}$ $nA \cdot T^{-1} \cdot Å^{-2}$), and the black arrows indicate the direction of the current flow for the same states.

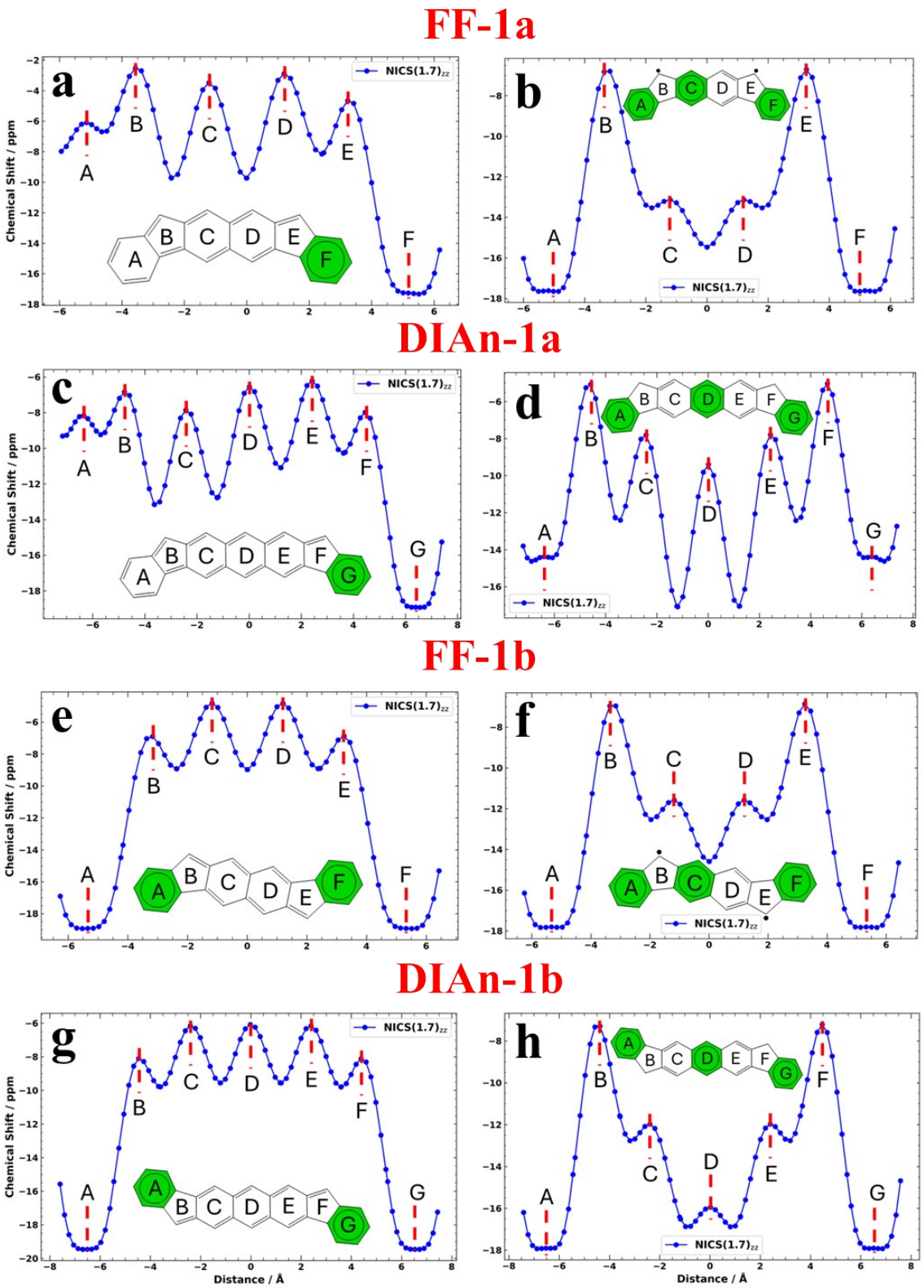

Figure S12. NICS-XY scan for CS (a)/(c)/(e)/(g), OS triplet (b)/(d) and singlet (f)/(h) states of **FF-1a/1b** and **DIAn-1a/1b** at a distance of 1.7 Å above the molecular plane.

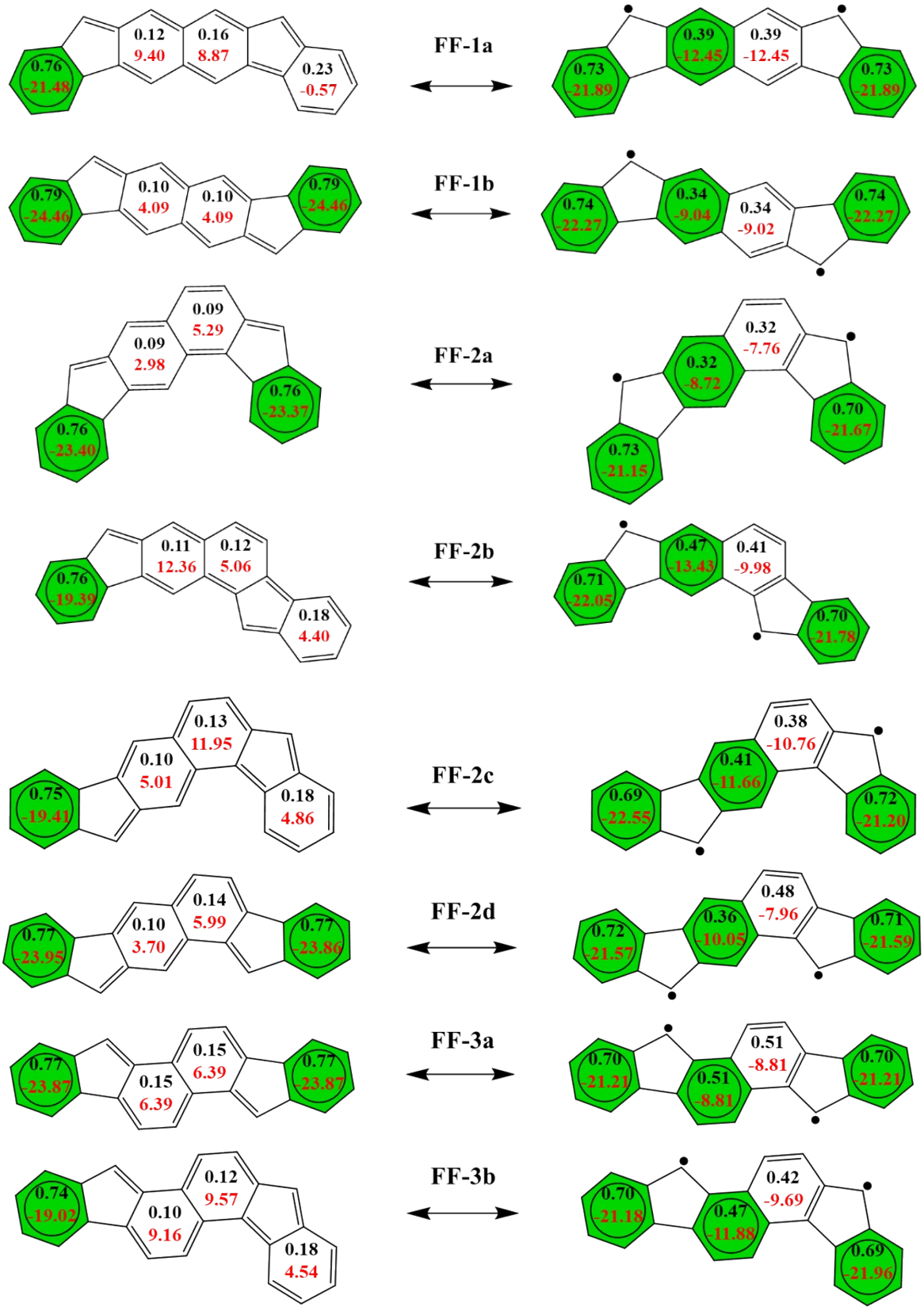
0.12
9.40
0.16
8.87
0.76
-21.48
0.23
-0.57
FF-1a
0.39
-12.45
0.39
-12.45
0.73
-21.89
0.73
-21.89
0.10
4.09
0.10
4.09
0.79
-24.46
0.79
-24.46
FF-1b
0.34
-9.04
0.34
-9.02
0.74
-22.27
0.74
-22.27
0.09
5.29
0.09
2.98
0.76
-23.37
0.76
-23.40
FF-2a
0.32
-7.76
0.32
-8.72
0.70
-21.67
0.73
-21.15
0.11
12.36
0.12
5.06
0.76
-19.39
0.18
4.40
FF-2b
0.47
-13.43
0.41
-9.98
0.71
-22.05
0.70
-21.78
0.13
11.95
0.10
5.01
0.75
-19.41
0.18
4.86
FF-2c
0.38
-10.76
0.41
-11.66
0.69
-22.55
0.72
-21.20
0.14
5.99
0.10
3.70
0.77
-23.95
0.77
-23.86
FF-2d
0.48
-7.96
0.36
-10.05
0.72
-21.57
0.71
-21.59
0.15
6.39
0.15
6.39
0.77
-23.87
0.77
-23.87
FF-3a
0.51
-8.81
0.51
-8.81
0.70
-21.21
0.70
-21.21
0.12
9.57
0.10
9.16
0.74
-19.02
0.18
4.54
FF-3b
0.42
-9.69
0.47
-11.88
0.70
-21.18
0.69
-21.96

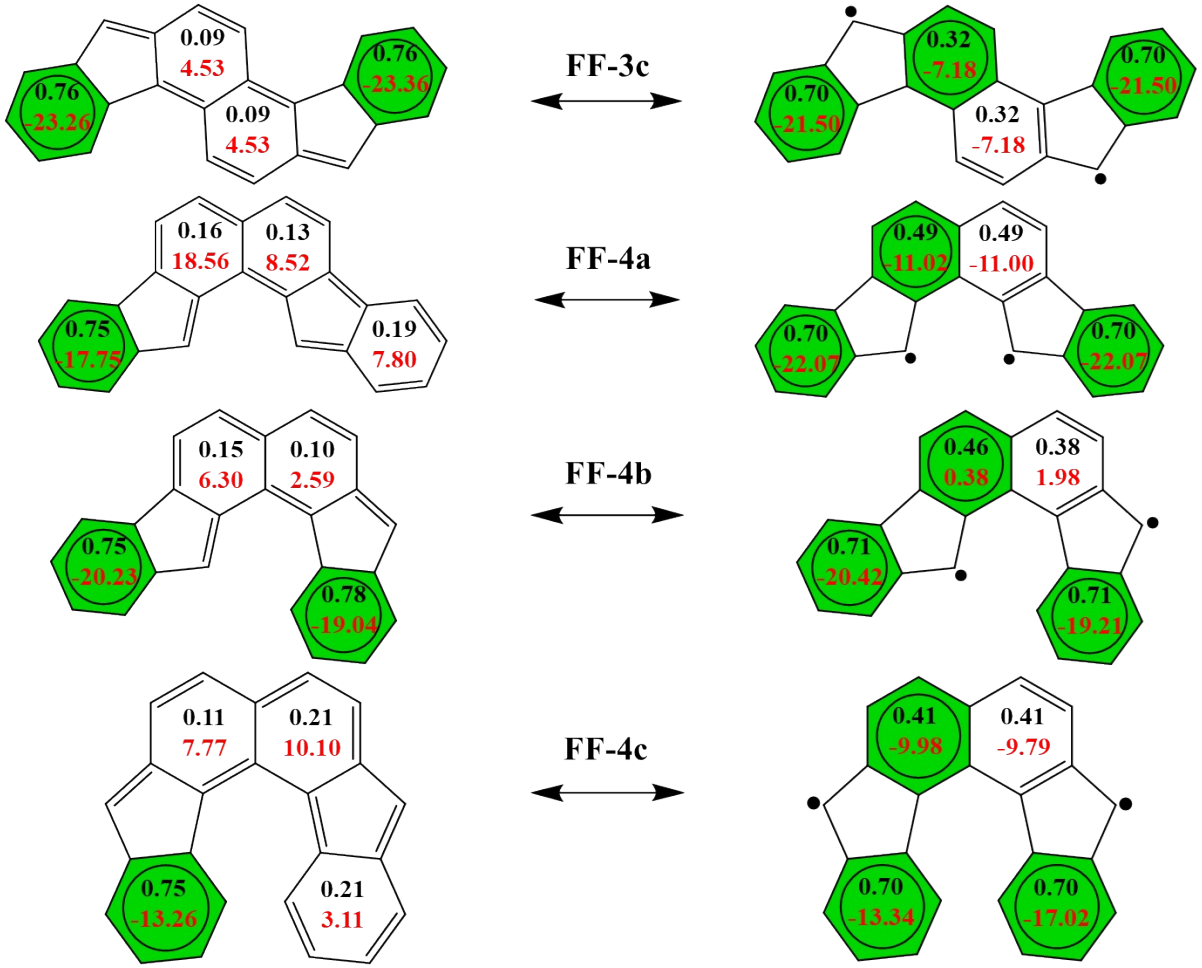

Figure S13. Normalized π-EDDB (numbers in black, electrons) and NICS(1)$_{zz}$ (numbers in red, ppm) values for CS and OS forms of **FF** isomers. Ring with a green color indicative of the Clar's aromatic π-sextets.

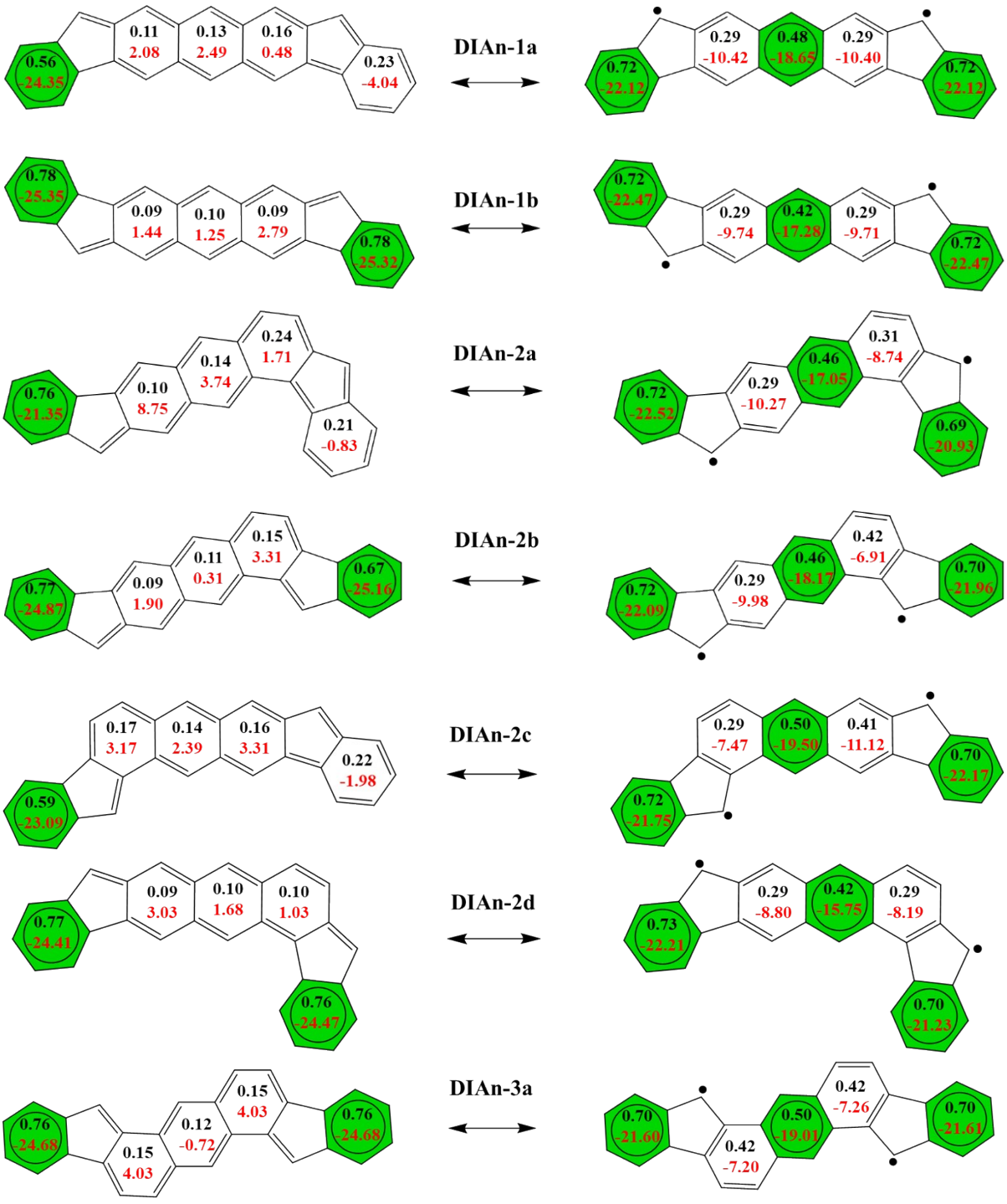
0.56
-24.35
0.11
2.08
0.13
2.49
0.16
0.48
0.23
-4.04
DIAn-1a
0.72
-22.12
0.29
-10.42
0.48
-18.65
0.29
-10.40
0.72
-22.12
0.78
-25.35
0.09
1.44
0.10
1.25
0.09
2.79
0.78
-25.32
DIAn-1b
0.72
-22.47
0.29
-9.74
0.42
-17.28
0.29
-9.71
0.72
-22.47
0.76
-21.35
0.10
8.75
0.14
3.74
0.24
1.71
0.21
-0.83
DIAn-2a
0.72
-22.52
0.29
-10.27
0.46
-17.05
0.31
-8.74
0.69
-20.93
0.77
-24.87
0.09
1.90
0.11
0.31
0.15
3.31
0.67
-25.16
DIAn-2b
0.72
-22.09
0.29
-9.98
0.46
-18.17
0.42
-6.91
0.70
-21.96
0.59
-23.09
0.17
3.17
0.14
2.39
0.16
3.31
0.22
-1.98
DIAn-2c
0.72
-21.75
0.29
-7.47
0.50
-19.50
0.41
-11.12
0.70
-22.17
0.77
-24.41
0.09
3.03
0.10
1.68
0.10
1.03
0.76
-24.47
DIAn-2d
0.73
-22.21
0.29
-8.80
0.42
-15.75
0.29
-8.19
0.70
-21.23
0.76
-24.68
0.15
4.03
0.12
-0.72
0.15
4.03
0.76
-24.68
DIAn-3a
0.70
-21.60
0.42
-7.20
0.50
-19.01
0.42
-7.26
0.70
-21.61

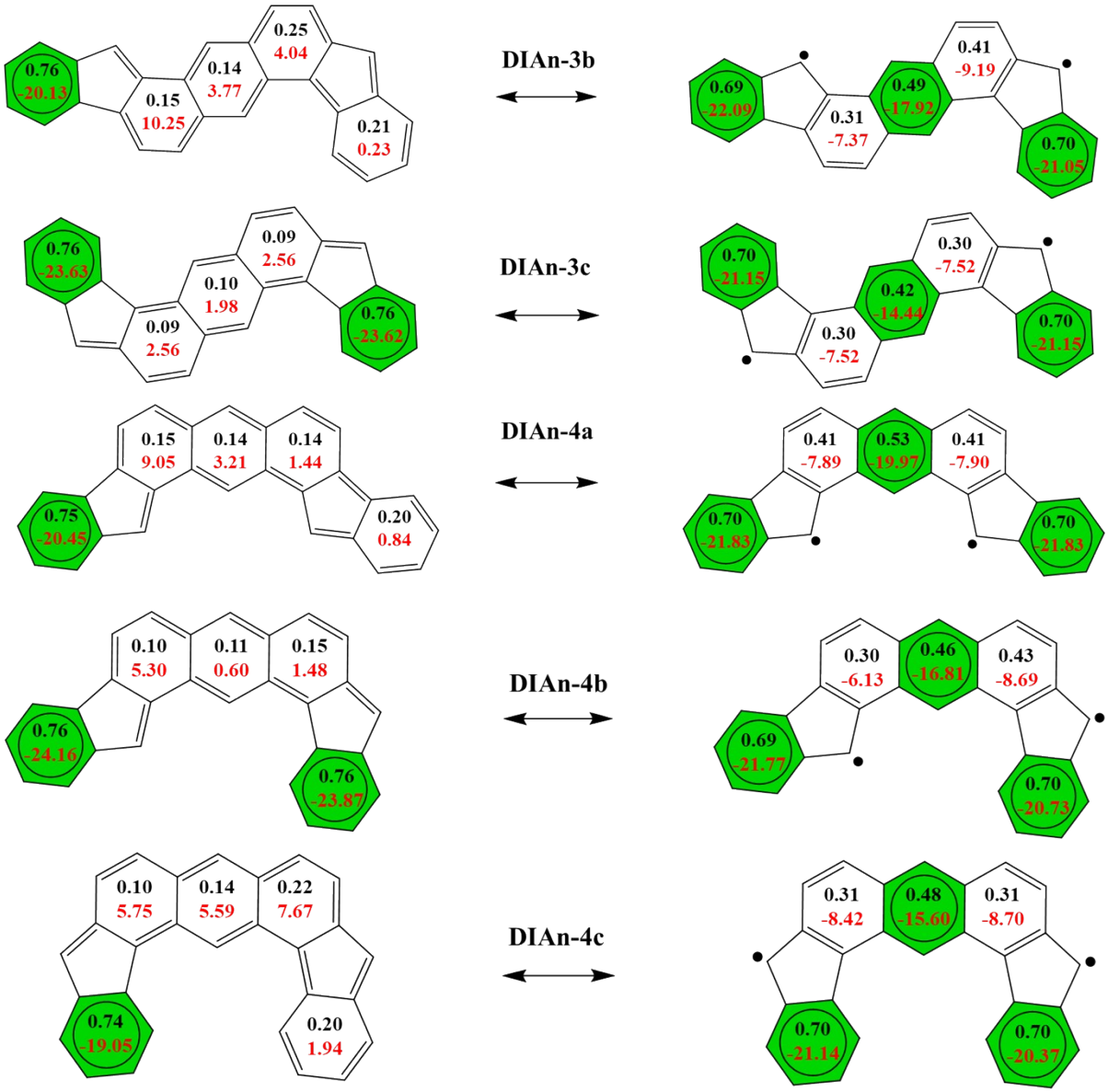

Figure S14. Normalized π-EDDB (numbers in black, electrons) and NICS(1)$_{zz}$ (numbers in red, ppm) values for CS and OS forms of **DIAn** isomers. Ring with a green color indicative of the Clar's aromatic π-sextets.

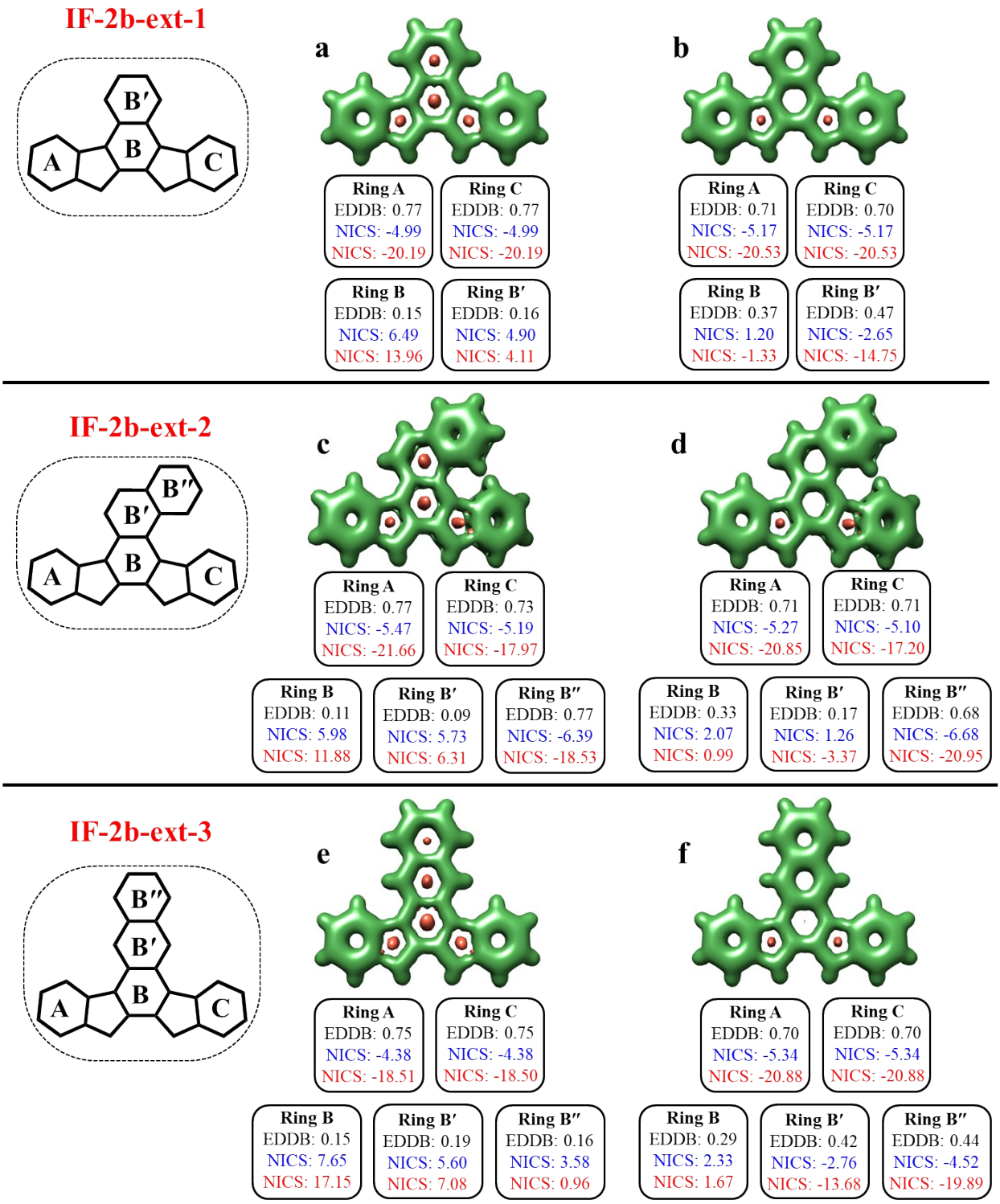

Figure S15. NICS(0)$_{iso}$ (numbers in blue, ppm), NICS(1)$_{zz}$ (numbers in red, ppm) values and 3D-NICS$_{iso}$ maps for CS (a)/(c)/(e), and OS singlet (b)/(d)/(f) states of **IF-2b-ext-1**, **IF-2b-ext-2** and **IF-2b-ext-3** plotted at [-11.0, 2.0] isovalues. Green and salmon color represents the shielded and deshielded regions.

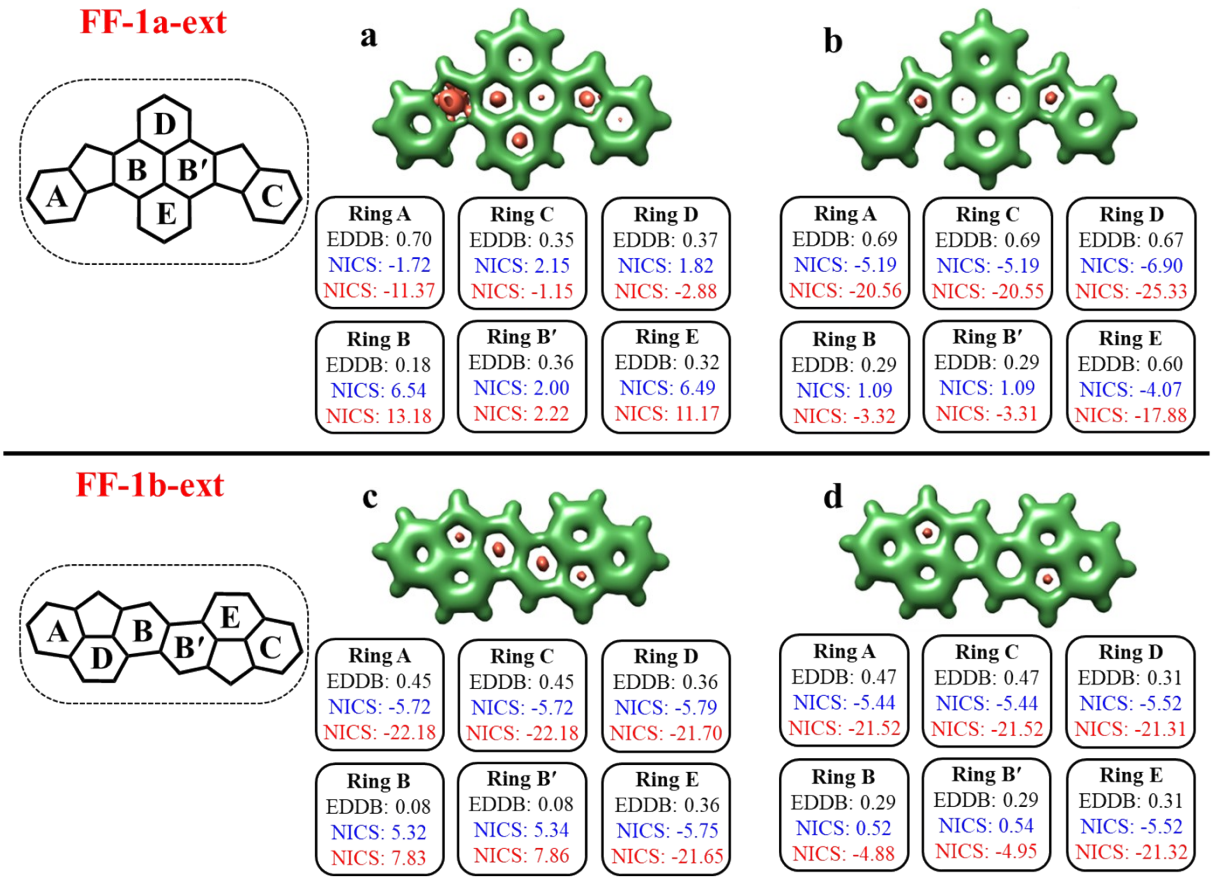

Figure S16. NICS(0)$_{iso}$ (numbers in blue, ppm), NICS(1)$_{zz}$ (numbers in red, ppm) values and 3D-NICS$_{iso}$ maps for CS (a)/(c), OS triplet (b), and singlet (d) states of **FF-1a-ext** (isovalues: [-11.0, 1.3]) and **FF-1b-ext** (isovalues: [-11.0, 2.0]). Green and salmon color pattern represents the shielded and deshielded regions.

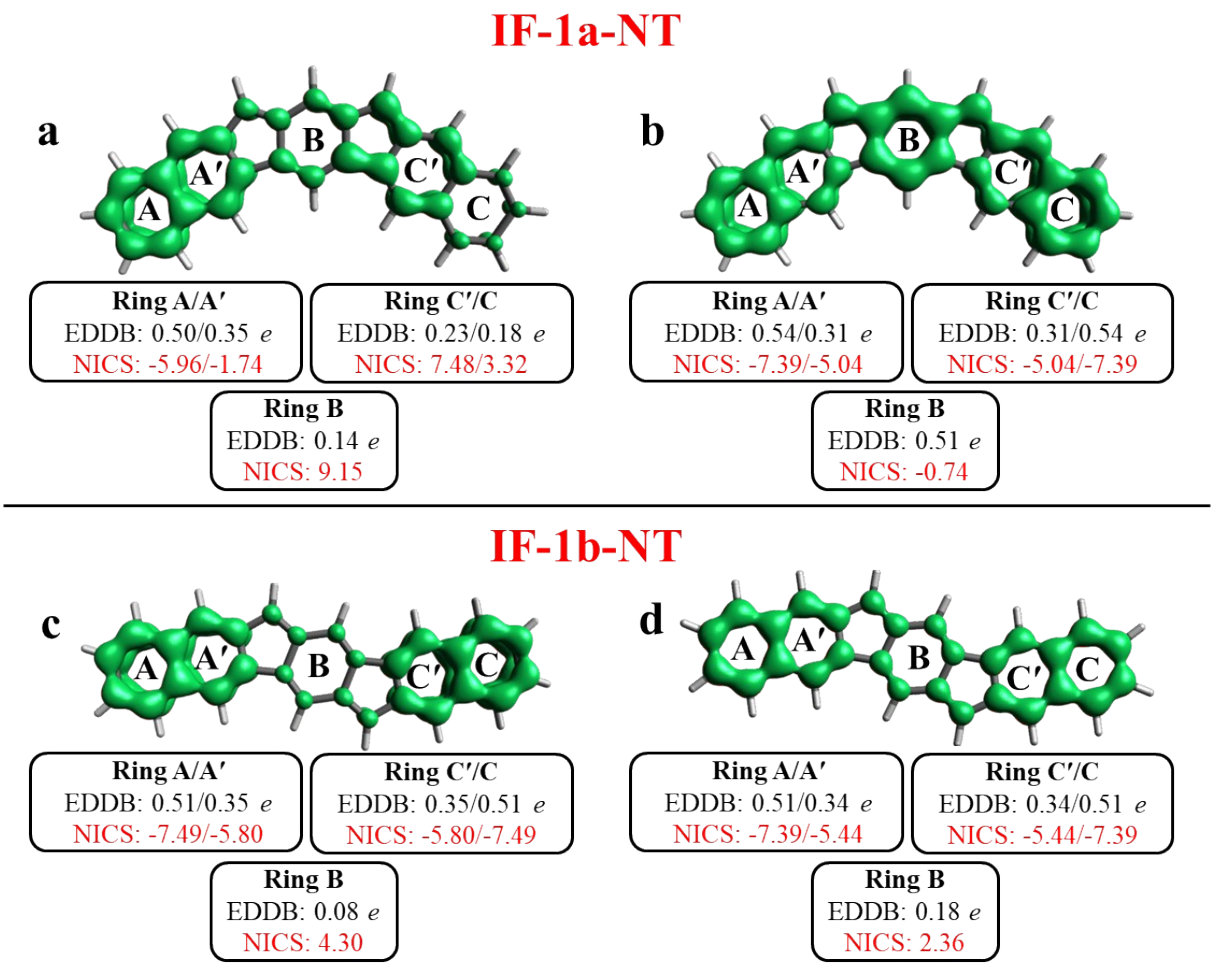

Figure S17. π-EDDB plots (isovalue: 0.015 e), normalized π-EDDB values, and NICS(0)$_{iso}$ (in ppm) for CS (a)/(c), OS triplet (b) and singlet (d) states of **IF-1a-NT** and **IF-1b-NT**.

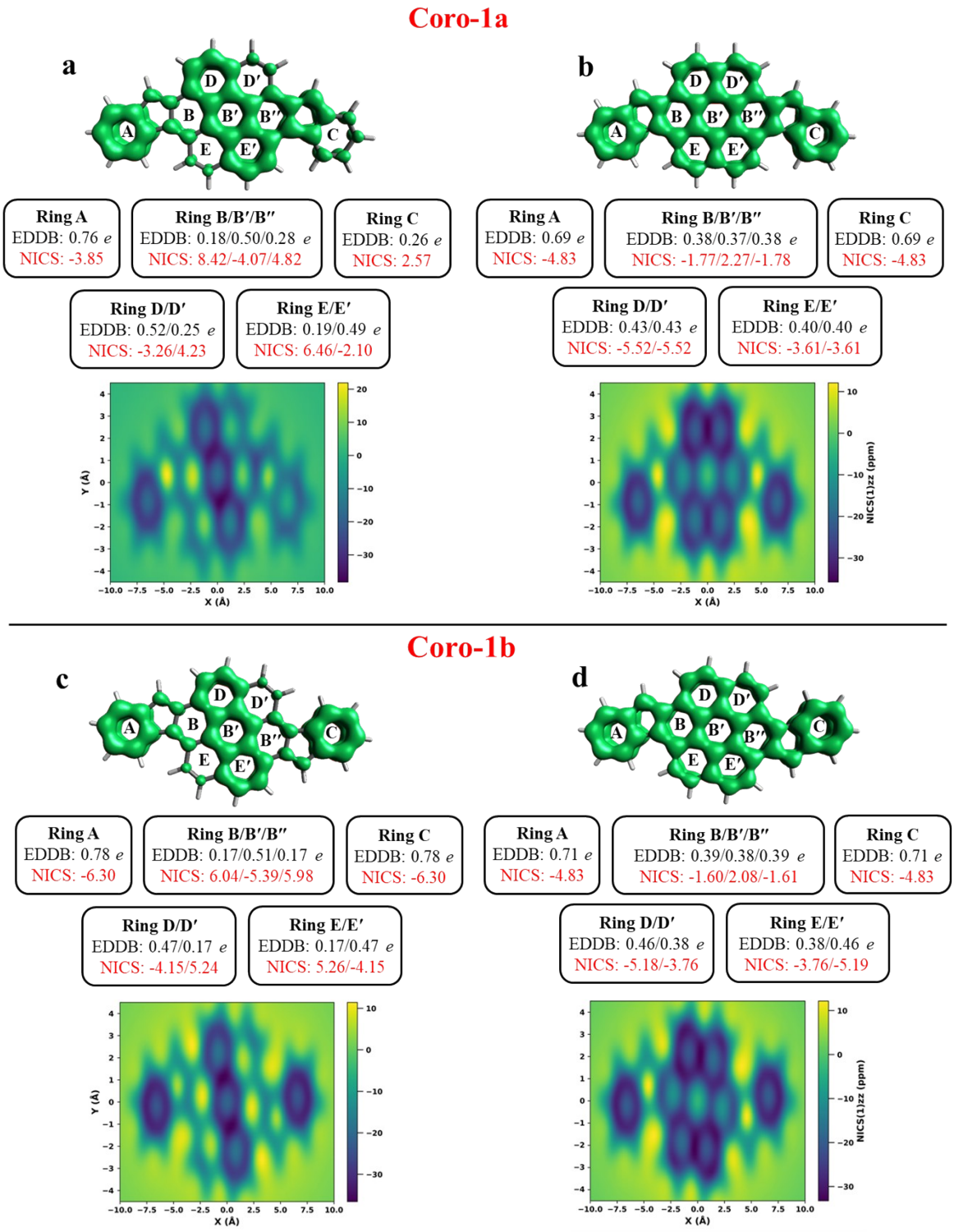

Figure S18. π-EDDB plots (isovalue: 0.015 e), normalized π-EDDB values, and NICS(0)$_{iso}$ (in ppm) for CS (a)/(c), OS triplet (b) and singlet (d) states, as well as corresponding 2D-NICS(1)$_{zz}$ scan of **Coro-1a** and **Coro-1b**.

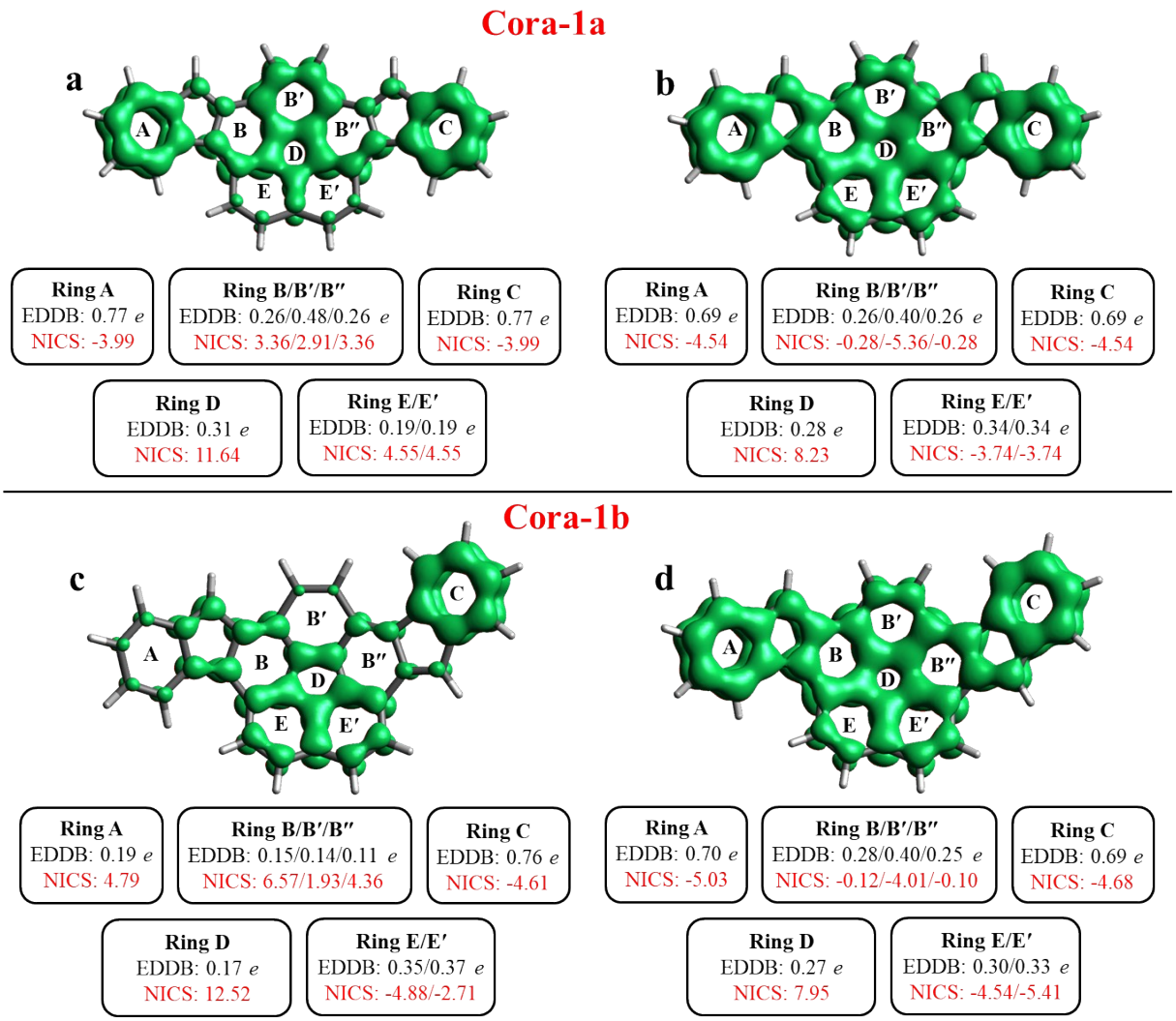

Figure S19. π-EDDB plots (isovalue: 0.015 e), normalized π-EDDB values, and NICS(0)$_{iso}$ (in ppm) for CS (a)/(c) and OS triplet (b)/(d) states of **Cora-1a** and **Cora-1b**.

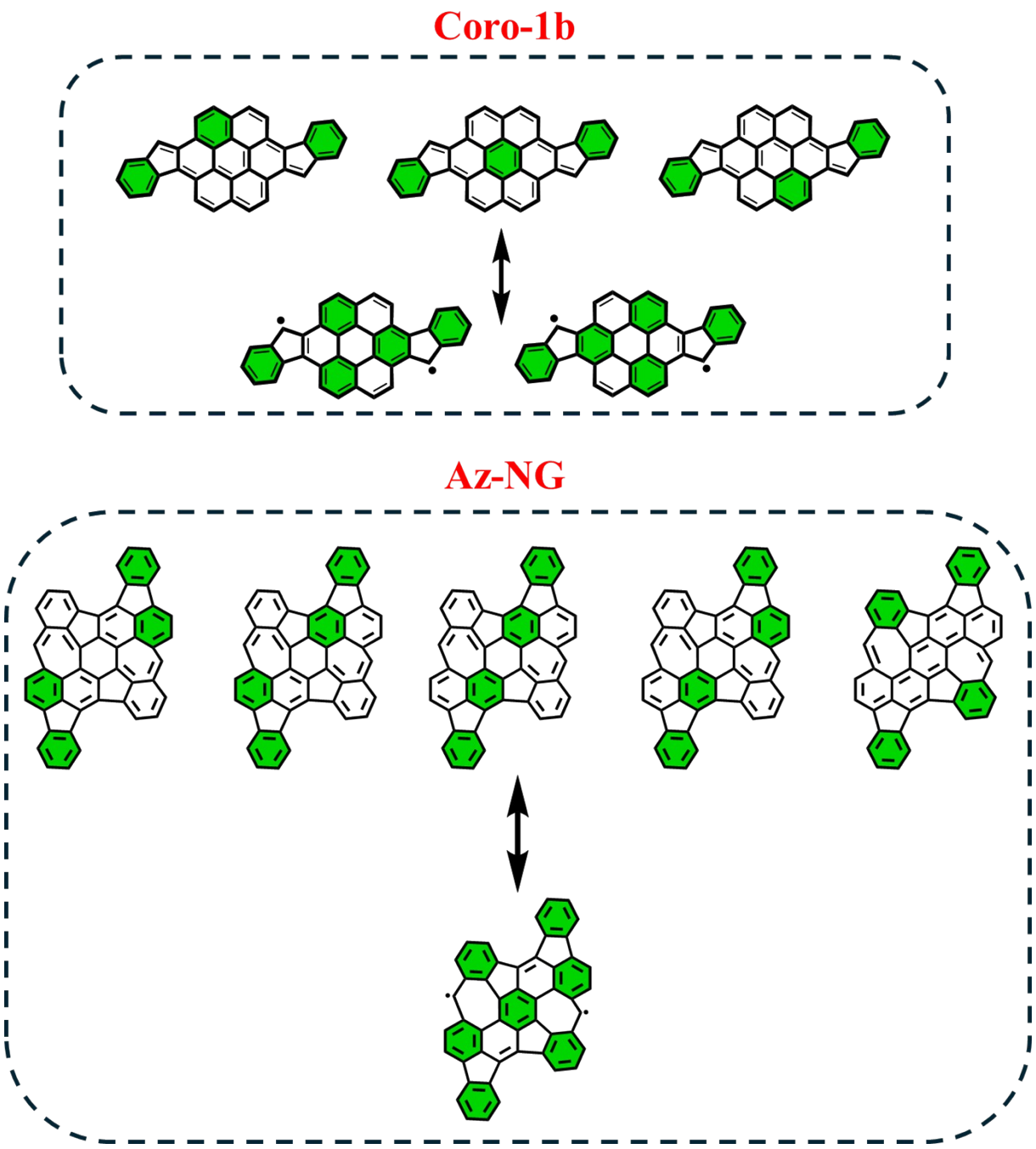

Figure S20. Clar resonators of **Coro-1b** and **Az-NG** in its closed and open-shell states. Clar's π-sextets are highlighted in green.

References

1. M. Nakano and B. Champagne, *J. Phys. Chem. Lett.*, 2015, **6**, 3236–3256.
2. D. Doehnert and J. Koutecky, *J. Am. Chem. Soc.*, 1980, **102**, 1789–1796.
3. S. Grimme and A. Hansen, *Angew. Chem. Int. Ed.*, 2015, **54**, 12308–12313.
4. A. Pérez-Guardiola, M. E. Sandoval-Salinas, D. Casanova, E. San-Fabián, A. J. Pérez-Jiménez and J. C. Sancho-García, *Phys. Chem. Chem. Phys.*, 2018, **20**, 7112–7124.
5. D. W. Szczepanik, *Comput. Theor. Chem.*, 2016, **1080**, 33–37.
6. E. D. Glendening, C. R. Landis and F. Weinhold, *J. Comput. Chem.*, 2019, **40**, 2234–2241.
7. M. Giambiagi, M. S. de Giambiagi and K. C. Mundim, *Struct. Chem.*, 1990, **1**, 423–427.
8. R. F. W. Bader, *Acc. Chem. Res.*, 1985, **18**, 9–15.
9. T. A. Keith, AIMAll, *TK Gristmill Software*, Vol. 2014.
10. E. Matito, *ESI-3D: Electron sharing Indexes Program for 3D Molecular Space Partitioning* 2015, Institute of Computational Chemistry and Catalysis, University of Girona, Catalonia, Spain.
11. A. Stanger, J. *Phys. Chem. A.*, 2019, **123**, 3922–3927.
12. M. Häser, R. Ahlrichs, H. P. Baron, P. Weis and H. Horn, *Theor. Chim. Acta.*, 1992, **83**, 455–470.
13. R. Gershoni-Poranne and A. Stanger, *Chem. – A Eur. J.*, 2014, **20**, 5673–5688.
14. J. Juselius, R. Bast, H. Fliegl, D. Sundholm, M. Dimitrova, L. Wirz, V. Liegeois, C. Kumar, T. Kjærgaard, J. Kussmann, J. Pyykkö, T. Järvinen and J. Gauss, 2023, *The gauge including magnetically induced current density method* (GIMIC) (2.2.1). Zenodo. https://doi.org/10.5281/zenodo.8183038
15. K. Wolinski, J. F. Hilton, and P. Pulay, *J. Am. Chem. Soc.*, 1990, **112**, 8251-8260.